

# STUDY ON THE APPLICATION OF WATER RESOURCE MANAGEMENT BASED ON GF-7 STEREO MAPPING SATELLITE

Ke Liu, LiRong Liu, ZhengYu Luo\*, YuHang Gan

Land Satellite Remote Sensing Application Center, Ministry of Natural Resources of P. R. China, Beijing, China

Corresponding author: 997610187@qq.com

**Keywords:** Water Resource, Remote Sensing, GF-7 Satellite, Stereo Mapping, Three-dimensional Dynamic Visualization.

## Abstract

GF-7 satellite was successfully launched on 3 Nov 2019. The two-line stereo camera can effectively obtain 20 km-width panchromatic stereo images with resolution better than 0.8m and 3.2m-resolution multispectral images. Through the composite mapping mode of stereo camera and laser altimeter, the satellite realizes 1:10,000-scale stereo mapping. This article selected the Qiafuqihai Reservoir and its upstream of the Yili River Basin as the study area. Hydrological landforms and vegetation coverage were monitored and three-dimensional dynamic simulation software was developed to verify the potential application of GF-7 stereo mapping satellite data in supporting drainage basin water resource allocation and management in future scenarios. 3 meters DSM derived from GF-7 surveying and mapping satellite finely portrayed the characteristics of hydroponic landforms of small watersheds. The upstream of Qiafuqihai was divided into eleven small watersheds. The water density was 8.5 times more than which was produced from STRM 90m. The elevation of the water-level fluctuation zone of the Qiafuqihai Reservoir ranged from 970 to 998 meters with the water area changed from 28.3 to 57.6 square kilometres. The terrain in the northwest and northeast was flat, with the main vegetation types being natural grasslands (64.9%) and arid lands (5.03%). The three-dimensional dynamic visualization software was developed and demonstrated hydrology information, vegetation coverage information and dynamic changes in the landform of the basin in three-dimensional environment. GF-7, the stereo surveying and mapping satellite, could be perfectly able to support the application of water resources deployment and management in the future.

## 1. Introduction

GF-7 satellite was successfully launched on 3 Nov 2019. Its lead user is the Ministry of Natural Resources of P. R. China (MNR), and it also serves other users, such as Ministry of Housing and Urban-Rural Development of P.R.China (MOHURD) and the National Bureau of Statistics(NBS).

GF-7 satellite runs on the sun-synchronous orbit and has a designed life of 8 years. The two-line stereo camera can effectively obtain 20 km-width panchromatic stereo images with resolution better than 0.8m and 3.2m-resolution multispectral images; the equipped two-beam laser altimeter can perform Earth observation at 3Hz observation frequency, with ground footprint diameter less than 30m, and acquire full waveform data at a sampling frequency higher than 1 GHz (Pi et al., 2023). Through the composite mapping mode of stereo camera and laser altimeter, the satellite realizes 1:10000-scale stereo mapping, serving the application needs of natural resource survey monitoring, basic surveying and mapping, and global geo-information resource construction, and providing high-precision satellite remote sensing images for the fields of housing and urban rural development as well as national survey statistics (Chen et al., 2023).

Sensor	Item	Parameter	
Bi-linear array stereo camera	Spectral Bands	Pan	0.45 ~ 0.90 $\mu\text{m}$
		MS	0.45 ~ 0.52 $\mu\text{m}$
			0.52 ~ 0.59 $\mu\text{m}$
			0.63 ~ 0.69 $\mu\text{m}$

Sensor	Item	Parameter		
		$\mu\text{m}$		
		0.77 ~ 0.89 $\mu\text{m}$		
	Forward inclination	+ 26°		
	Backward inclination	- 5°		
	Resolution	Pan	Backward panchromatic :0.65m	
		MS	Forward panchromatic :0.8m	
	Swath Width	$\geq 20$ km		
	Laser Altimeter	Laser beam	2 beams	
Laser repetition frequency		3Hz		
Range Accuracy		$\leq 0.3$ m (Gradient less than 15°)		
Single pulse energy		$\leq 180$ mJ		
Laser Wavelength		1.064 $\mu\text{m}$		
Facular Size		30 m		
Sensor Footprint	Laser Divergence Angle	$\leq 60$ $\mu\text{rad}$		
	Spectral Bands	0.50~0.72 $\mu\text{m}$ 1.064 $\mu\text{m}$		
	Ground Pixel Resolution	$\leq 4$ m		
	Viewing field	+0.6° ~ +0.8°		

Sensor	Item	Parameter
		- 0.6° ~ - 0.8°
	Swath Width	1.6 km

Table 1. Sensor technical parameters of GF-7.

This article selected the Qiafuqihai Reservoir and its upstream of the Yili River Basin as the study area. Hydrological landforms and vegetation coverage were monitored and three-dimensional dynamic simulation software was developed to verify the potential application of GF-7 stereo mapping satellite data in supporting drainage basin water resource allocation and management in future scenarios.

## 2. Study Area

The Yili River is the largest river in Xinjiang. It originates from the north side of Khan Tengri Peak in the Tianshan Mountains of China and merges into Lake Balkhash in Kazakhstan. The total length of the river is 1,236 kilometres and the drainage area is 151,000 square kilometres. The river length in China is 442 kilometres and the drainage area is 56,000 square kilometres. It is the main water source of Balkhash Lake in Kazakhstan.

Since the beginning of the 21st century, Xinjiang's meteorology and hydrology have generally shown a "warm and humidification" phenomenon, with precipitation and runoff increasing significantly. At the same time, Xinjiang's economic and social development faces important opportunities, and water resources are a rigid constraint for industrial development, urban construction and ecological protection. Economic and social development and ecological environmental protection urgently need to be compatible with the carrying capacity of water resources and the environment. Affected by the comprehensive impacts of climate change, human activities, etc., the development and utilization of water resources in the Yili River Basin is facing new challenges (Wang et al., 2017).

Up to now, there is a lack of key water information products for remote sensing in the Yili River Basin. The high-resolution remote sensing image products of the GF-7 satellite were used to analyse the topography and hydrological characteristics of the basin, which could provide a basis for subsequent water resource allocation in the basin and provide continuous technical support to ensure the economic development and ecological protection of the river basin. The study area of this article is in the Qiafuqihai Reservoir and its upstream of the Yili River Basin, with an area of 6047 square kilometres (Figure 1).

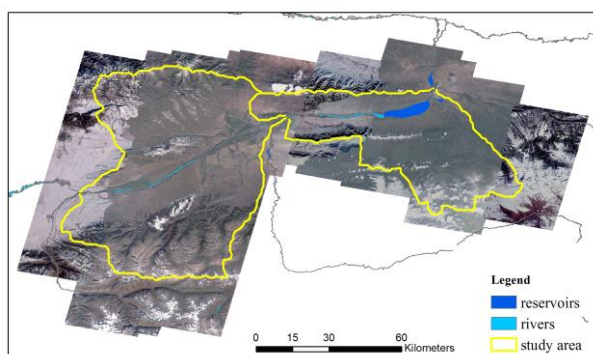


Figure 1. Schematic diagram of the study area.

## 3. Data Source

### 3.1 Remote Sensing Images and Processing

A total of seventy-eight scene images including multispectral images, forward and backward panchromatic images of GF-7 satellite were collected. Panchromatic and multispectral images of GF-2 satellite were also collected in order to supplement data gaps. Firstly, eighty-six control points at the scale 1:10,000 were collected through the field work to obtain block network development and a three-dimensional model (d'Angelo, et al., 2023). Secondly, semi-global matching method based on geometric constraints was used for cloud-dense matching (Tang et al., 2020). Thirdly, DSM (Digital Surface Model) of 3 meters resolution and DOM (Digital Orthophoto Map) of 0.8 meters resolution were produced after orthorectification, clipped, mosaiced processing (Figure 2).

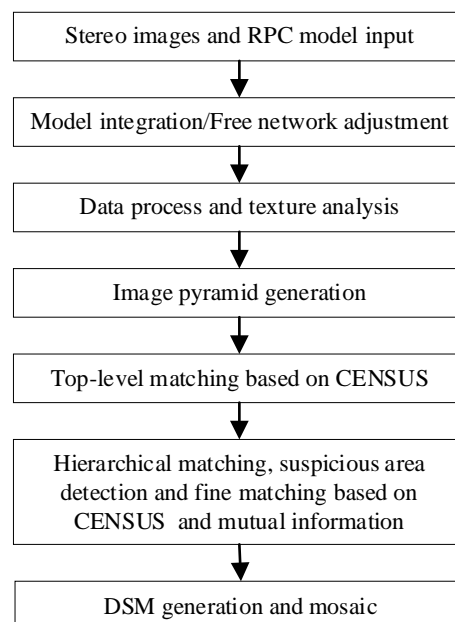


Figure 2. Flow chart of DSM extraction based on GF-7 stereo images.

### 3.2 Thematic Data

Thematic data including hydrology and water conservancy data were also integrated in this research.

## 4. Research Methods

### 4.1 Hydrological Parameter Extraction

High-precision basin division was carried out using digital terrain analysis technology through key steps such as depression, flow calculation, flow accumulation calculation, water system extraction, and basin extraction (Figure 3).

**4.1.1 Depression filling:** Due to the influence of data noise and interpolation methods, DEM data often contains some "depressions" which will cause poor water flow in the basin and cannot form a complete drainage network. Therefore, when using simulation methods to analyze the drainage basin topography, we must first process the depressions in the DEM data. Depression filling is the basis of watershed analysis.

**4.1.2 Flow direction calculation:** The flow direction is the direction in which water flows as it leaves this grid. Multi-flow direction algorithm is used to calculate the direction of water flow. The multi-flow direction algorithm directs runoff to several relatively low adjacent cells in a certain proportion. Use the D8 algorithm to determine the direction of water flow. First, calculate the slope and aspect relationship between each grid unit of the DEM data and its surroundings. Then select the steepest slope and set the steepest slope as the water flow direction of the unit. In each grid unit, There are 8 possible directions for the water to flow around, and the 8 flow direction codes of 1, 2, 4, 8, 16, 32, 64, and 128 are used to represent each outflow direction. By comparing the slope, select a certain direction to determine the direction of the water flow.

**4.1.3 Flow accumulation calculation:** The water flow accumulation matrix represents the cumulative amount of water flow at each grid point. After determining the direction of the water flow and the distribution of water volume, it can be obtained by using the regional topographic water flow simulation method. The following takes the D8 method as an example to briefly introduce its basic idea: Assume that there is 1 unit of water volume at each grid point. According to the D8 algorithm, the direction of the water flow at each grid point is obtained. According to the natural law of water flow from high to low, the cumulative water volume of each grid is calculated. An iterative method can be used in algorithm design.

Use the Flow Accumulation function under the ArcGIS hydrological analysis module to determine the catchment of the basin water system, set the raster critical value, identify the number of effective rasters, calculate the number of accumulated catchment rasters on the effective raster, and determine the catchment area and cumulative amount of catchment. is the sum of the number of grid cells multiplied by the area of the grid cells. The number of effective grids identified by calculation can represent the converging capacity of the watershed system. That is, the greater the number of converging grids in a certain watershed unit, the larger the converging area formed, and the more obvious the surface runoff is.

**4.1.4 Basin water system extraction:** It is based on the cumulative amount of catchment and is extracted by setting a certain threshold. Grid cells at this threshold are connected along the flow direction to form a watershed network. Since the exported basin water system is raster data, the extracted raster data also needs to be converted into vector data.

Based on the runoff overflow model, the water system is generated by simulating the flow of surface runoff, and then the water dividing line can be determined and the watershed can be divided. This method mainly determines the flow direction based on the maximum slope between the DEM grid unit and eight adjacent cells, and calculates the upstream confluence capacity of each cell.

Extracting watersheds in ARCGIS is actually to directly select the minimum number of rasters that flow into the watershed, and automatically generate sub-watersheds. The extraction process is as follows: first, fill in and peak the DEM data, and then based on the flow direction of each raster unit, the confluence capacity of each grid unit is calculated. The threshold method is used to determine the river network based on the confluence capacity. Finally, all sub-basins are quickly identified through the river network and water outlets.

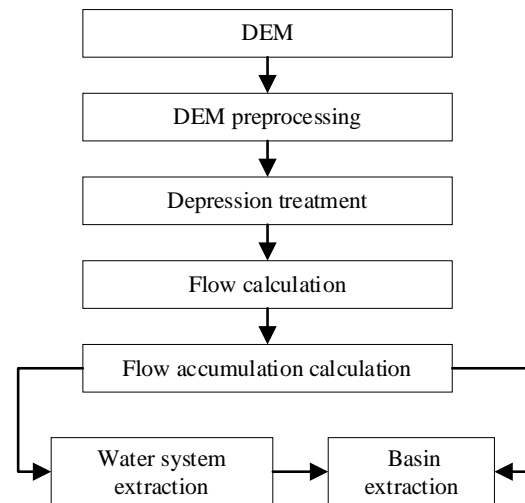


Figure 3. Flow chart of water system and basin extraction.

## 4.2 Vegetation Coverage Information Extraction

Moreover, the water-level fluctuation zone of the Qiafuqihai Reservoir was extracted based on 3 meters resolution DSM and hydrological data. Vegetation coverage information was produced in a three -dimensional environment using remote sensing information extraction technology.

## 4.3 3D Dynamic Software Development

3D dynamic software was developed to achieve dynamic changes in landforms using DOM, DSM, and thematic data generated from GF-7 stereo mapping satellite based on Dragon Map platform. Dragon Map is a dynamic 3D geographic information system with completely independent intellectual property rights that developed by Satellite Surveying and Mapping Application Center, NASG (Figure 4).

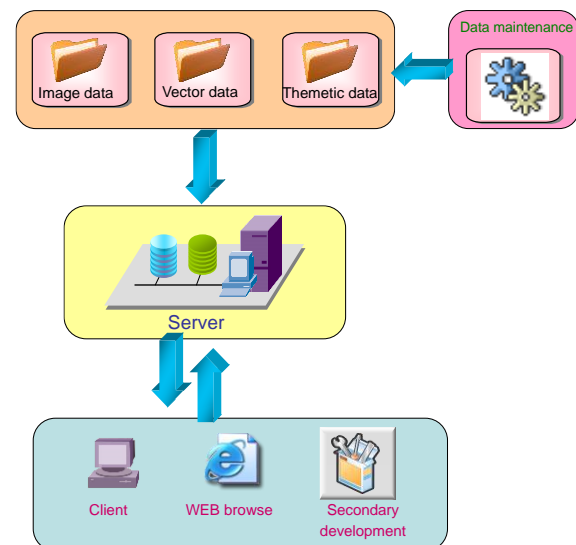


Figure 4. System architecture diagram of dragon map.

The system involves dynamic 3D visualization platform, server data dissemination platform and application development software package. It is a dynamic 3D geographic information platform providing a series of dynamic services, such as rapid integration and browse of multi-source heterogeneous data, multi-temporal data contrast, statistical analysis and dynamic

load of multimedia information. It supports fast loading of massive multi-source heterogeneous data, including image data, vector data, terrain models, multimedia data and other network data services. It Supports inversion of temporal dynamic changes for topography, terrain and regional polygon based on multi-temporal images, elevation, vector data. It provide red / blue stereo and time-division 3D mode to reach more realistic virtual simulation of landforms and models of 3D surface features.

## 5. Results and Analysis

### 5.1 Small watershed and water system analysis

The upstream of Qiafuqihai was divided into eleven small watersheds. 3 meters DSM derived from GF-7 surveying and mapping satellite finely portrayed the characteristics of hydroponic landforms of small watersheds.

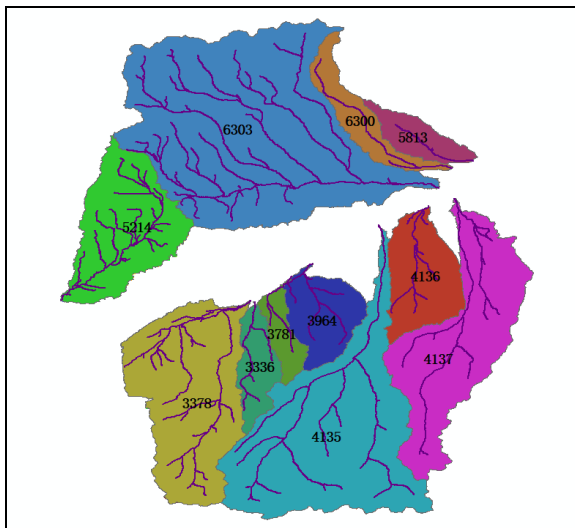


Figure 5. Small watersheds coding of the study area.

Watershed Number	Code	Area (square meters)
1	3336	81570220.41
2	3378	410252863.8
3	3781	51336447.12
4	3964	123560961.5
5	4135	598383019.4
6	4136	162796079.4
7	4137	382262382.7
8	5214	268372872.9
9	5813	67193722.66
10	6300	97847638.72
11	6303	886606771.5

Table 2. Small watersheds area statistics of the study area.

We simply used 4 digits to number the watersheds in the study area. The extraction of small watersheds and their corresponding numbers are shown in Figure 5. The area of each small watershed in the extracted demonstration area was statistically calculated, as shown in Table 2. The largest small

watershed was No. 6303 watershed, with an area of 886606771.5 square meters.

Further more, water syestem derived from 3m DSM of GF-7 and SRTM 90m were compared by river network density. River network density is the ratio of total length of rivers in the basin to basin area. The water density was 8.5 times more than which was produced from STRM 90m (Figure 6 ).

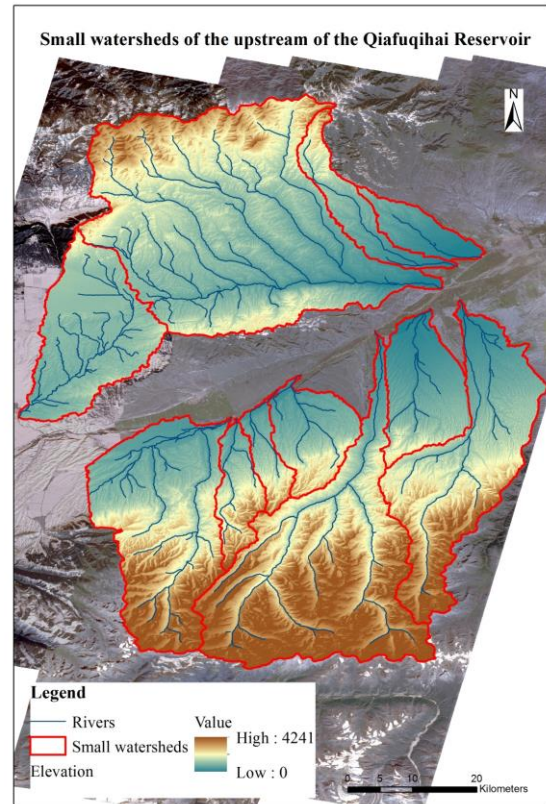


Figure 6. Small watersheds and rivers derived from DSM of GF-7 stereo satellite.

### 5.2 Vegetation Coverage analysis

The elevation of the water-level fluctuation zone of the Qiafuqihai Reservoir ranged from 970 to 998 meters with the water area changed from 28.3 to 57.6 square kilometres. The Qiafuqihai Reservoir fluctuation zone covered an area of 29.29 square kilometers. The main land types were grassland and mudflat land. The area and propportion are shown in Table 3.

Vegetation coverage types	Area (square kilometers)	Ratio
Arable land	1.50	5.03%
Bare rock	1.83	6.13%
Mudflat	7.16	23.94%
Natural grassland	19.42	64.90%

Table 3. Area statistics of each vegetation coverage type in the study area.

The grasslands were all natural grasslands, mainly concentrated in the northwest of the Qiafuqihai Reservoir, with a small amount distributed in the northeast. From the GF-7 satellite remote sensing images in three-dimensional view, it was known



that the northwest and northeast of the Qiafuqihai Reservoir flat and were the alluvial fan area of the Tekes River. It was suitable for the growth of natural grassland.

All water areas and facility lands were tidal flats, and their distribution areas were the same as those of natural grasslands. All other land was bare rocky gravel land, mainly distributed in the northern part of the Qiafuqihai Reservoir and the narrow water area. According to the three-dimensional images obtained from the GF-7 satellite remote sensing images, the terrain in the northern part of the Qiafuqihai Reservoir and the narrow water area was steep, all bare rocky gravel land.

All cultivated land was dry land, mainly concentrated in the northwest of the Chapqi Sea, with a small amount distributed in the northeast. Its distribution area was the same as that of natural grassland, which was obtained from the GF-7 satellite remote sensing image in three dimensions. Compared with the natural grassland in Qiafuqihai, the terrain was higher, flatter, closer to the road, more convenient for reclamation, and lower in production costs (Figure 7).

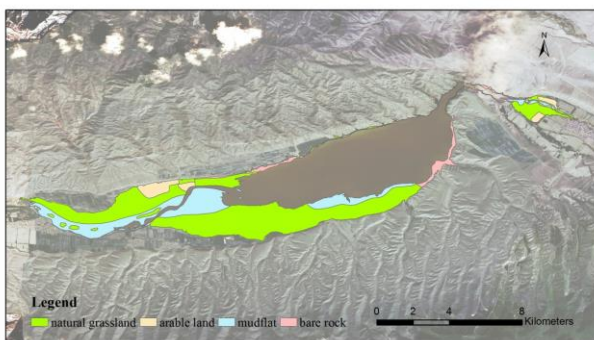


Figure 7. Vegetation cover extracted from GF-7 stereo satellite in the water-level fluctuation zone of the Qiafuqihai Reservoir.

### 5.3 3D Dynamic Software

The three-dimensional dynamic visualization software was developed and demonstrated hydrology information, vegetation coverage information and dynamic changes in the landform of the basin in three-dimensional environment (Figure 8-10). The software also supported the water diversion route planning and route length calculation. GF-7, the stereo surveying and mapping satellite, could be perfectly able to support the application of water resources deployment and management in the future.

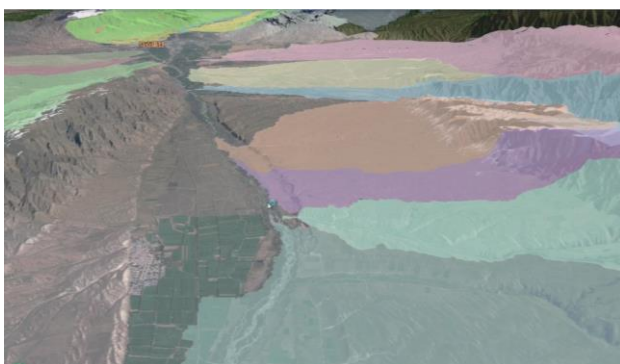


Figure 8. Small watersheds demonstrated by the three - dimensional dynamic visualization software.

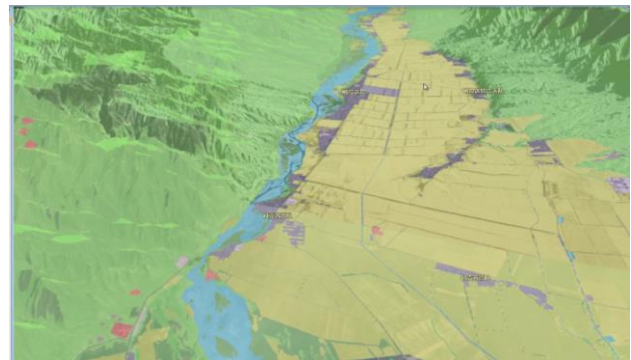


Figure 9. Vegetation coverage demonstrated by the three - dimensional dynamic visualization software.

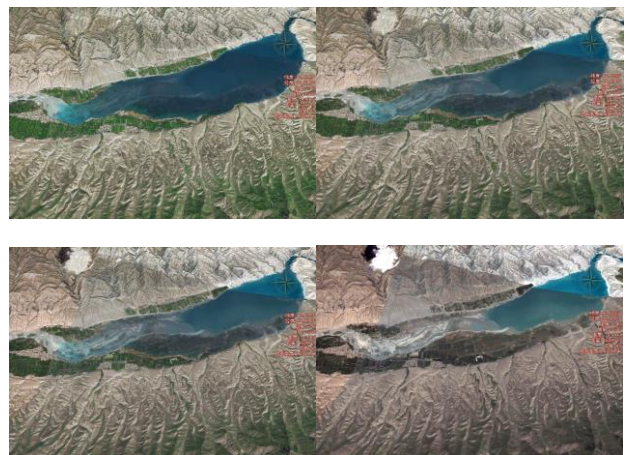


Figure 10. Dynamic changes in the landform demonstrated by the three - dimensional dynamic visualization software.

## 6. Conclusions and Discussions

The GF-7 three-dimensional satellite mapping data can accurately depict the hydrological and geomorphological characteristics of the basin. The three-dimensional environment provided supported the high-precision acquisition of micro-topographic information on water resources and water conservancy facilities at a scale of 1:10,000. It can provide key support for the planning and management of water and land resources in the basin. It has the application capabilities to support basin water resources allocation management under future scenarios.

In the future, we can further explore the application potential of high-resolution three-dimensional mapping satellites by further combining application needs such as smart water conservancy construction, digital watershed construction, hydrological modeling of no/missing data areas, digital scene construction, and digital twin watershed construction.

### Acknowledgements

This work was supported by National Key R&D Program of China "Joint Research, Development and Application Demonstration of Remote Sensing Monitoring Technology for Typical Natural Resources Features" (Grant No. 2023YFE0207900).

### References

Chen, P., Huang, H., Liu, J., Wang, J., Liu, C., Zhang, N., & Zhang, D., 2023. Leveraging Chinese GaoFen-7 imagery for high-resolution building height estimation in multiple cities. *Remote Sensing of Environment*, 298, 113802. doi.org/10.1016/j.rse.2023.113802.

d'Angelo, P., & Tian, J., 2023. Geometric evaluation of gaofen-7 stereo data. *ISPRS Annals of the Photogrammetry, Remote Sensing and Spatial Information Sciences*, 10, 805-811. doi.org/10.5194/isprs-annals-X-1-W1-2023-805-2023.

Pi, Y., Yang, B., Li, X., & Wang, M., 2022. Robust correction of relative geometric errors among GaoFen-7 regional stereo images based on posteriori compensation. *IEEE Journal of Selected Topics in Applied Earth Observations and Remote Sensing*, 15, 3224-3234. doi.org/10.1109/JSTARS.2022.3169474.

Tang, X., Xie, J., Liu, R., Huang, G., Zhao, C., Zhen, Y., & Dou, X., 2020. Overview of the GF-7 laser altimeter system mission. *Earth and Space Science*, 7(1), e2019EA000777. doi.org/10.1029/2019EA000777.

Wang, Y. J., & Qin, D. H., 2017. Influence of climate change and human activity on water resources in arid region of Northwest China: An overview. *Advances in Climate Change Research*, 8(4), 268-278. doi.org/10.1016/j.accre.2017.08.004.